ResearchGate

See discussions, stats, and author profiles for this publication at: https://www.researchgate.net/publication/45917421

Slime mould logical gates: exploring ballistic approach

Article · May 2010

Source: arXiv

CITATIONS
64

READS
58

1 author:

Andrew Adamatzky
University of the West of England, Bristol
608 PUBLICATIONS **7,570** CITATIONS

SEE PROFILE

Some of the authors of this publication are also working on these related projects:

Project Reversible Cellular Automata View project

Project Unconventional Computing View project

All content following this page was uploaded by Andrew Adamatzky on 17 October 2014.

The user has requested enhancement of the downloaded file.

arXiv:1005.2301v1 [nlin.PS] 13 May 2010

Slime mould logical gates: exploring ballistic approach

Andrew Adamatzky

University of the West of England, Bristol, United Kingdom
andrew.adamatzky@uwe.ac.uk

Abstract

Plasmodium of *Physarum polycephalum* is a single cell visible by unaided eye. On a non-nutrient substrate the plasmodium propagates as a traveling localization, as a compact wave-fragment of protoplasm. The plasmodium-localization travels in its originally predetermined direction for a substantial period of time even when no gradient of chemo-attractants is present. We utilize this property of *Physarum* localizations to design a two-input two-output Boolean logic gates $\langle x, y\rangle \to \langle xy, x+y\rangle$ and $\langle x, y\rangle \to \langle x, \overline{x}y\rangle$. We verify the designs in laboratory experiments and computer simulations. We cascade the logical gates into one-bit half-adder and simulate its functionality.

Keywords: *Physarum polycephalum*, logical gate, adder, unconventional computer, chemical computer, biological computer

1 Introduction

Plasmodium of *Physarum polycephalum* is a single cell with many diploid nuclei. The cell is visible by naked eye and can grow up to meters when properly cared for. The plasmodium feeds on microscopic food particles, including microbial life forms. The plasmodium placed in an environment with distributed nutrients develops a network of protoplasmic tubes spanning the nutrients' sources.

In its foraging behavior the plasmodium approximates shortest path [13], computes planar proximity graphs [5] and plane tessellations [16], exhibits primitive memory [15], realizes basic logical computing [17], and controls robot navigation [18]. The plasmodium can be considered as a general-purpose computer because the plasmodium simulates Kolmogorov-Uspenskii machine — the storage modification machine operating on a labeled set of graph nodes [4].

In 2004 Tsuda, Aono and Gunji [17] demonstrated in laboratory experiments realisation of Boolean logic negation and conjuction by plasmodium of *Physarum polycephalum*. In 2004 Adamatzky and De Lacy Costello esablished in numerical simulation [3] and chemical laboratory experiments [9] that by colliding localized excitations, or wave-fragments, in excitable chemical medium one can implement functionally complete set of logical gates. We merge approaches [17] and [3,9] in present paper. We adapt concepts of collision-based computing [2] to realms of Physarum behaviour, and develop experimental prototypes of two-input two-output Boolean logical gates.

The paper is structured as follows. Methods of cultivating and experimenting with plasmodium of *Physarum polycephalum* are described in Sect. 2. In Sect. 3 we provide experimental evidence of 'ballistic' behavior of traveling plasmodium localizations. Experimental Physarum gates are discussed in Sect. 4. In Sect. 5 experimental results are supported by numerical simulation of propagating localizations. The gates are cascaded in one-bit half-adder in Sect. 6. Importance of non-nutrient substrate for gate implementation is highlighted in Sect. 7.

2 Materials and Methods

Plasmodium of *Physarum polycephalum* is cultivated in large plastic boxes, on a wet paper towels and fed with oat flakes. Experiments are conducted in round Petri dishes (9 cm in diameter) and rectangular Petri dishes (12 cm $\times$ 12 cm). Channels and junctions physically representing logical gates are cut of a non-nutrient 2% agar plates (Select agar, Sigma Aldrich). The dishes are kept in room temperature (c. 25^o) in darkness. Images of plasmodium propagating in Petri dishes are taken by Epson Perfection 4490 scanner, resolution 600. Colors are enhanced by increasing saturation and contrast.

We use two-variable Oregonator model to numerically simulate propagation of plasmodium localizations. Our choice and details of the model are outlined below.

Localized excitations in sub-excitable Belousov-Zhabotinsky (BZ) medium behave similarly to pseudopodia of *P. polycephalum* [6,7]. Sources of nutrients are chemo-attractants for plasmodium, gradients of shade are 'photo-attractants' for excitation waves in BZ medium. In [7] we shown how to navigate traveling localizations and growing parts of plasmodium by spatial configuration of attractants. We adopt the analogy developed in [7] and simulate propagating plasmodium using two-variable Oregonator equation [10] adapted to a light-sensitive BZ reaction with applied illumination [8]:

$$\frac{\partial u}{\partial t} = \frac{1}{\epsilon}(u - u^2 - (fv + \phi)\frac{u - q}{u + q}) + D_u \nabla^2 u$$
$$\frac{\partial v}{\partial t} = u - v.$$

In framework of BZ reaction the variables u and v represent local concentrations of activator, or excitatory component, and inhibitor, or refractory component. With regards to plasmodium of *P. polycephalum* activator, u, is analogous to concentration, or 'thickness', of the plasmodium's cytoplasm at the propagating pseudopodium. Inhibitor, v, combines several factors, when plasmodium is concerned. These factors include rate of nutrients consumption, byproducts of biochemical chains ignited by signals on photo- and chemoreceptors, and concentration of metabolites released by the plasmodium into its substrate.

Parameter ϵ sets up a ratio of time scale of variables u and v, q is a scaling parameter depending on rates of activation/propagation and inhibition, f is a stoichiometric coefficient. Constant ϕ is a rate of inhibitor production. In light-sensitive BZ ϕ represents rate of inhibitor production proportional to intensity of illumination. In terms of plasmodium ϕ represents rate of inhibitor proportional to concentration of nutrients, metabolites, illumination, chemical repellents. See detailed comparison of BZ and Physarum in [6,7].

To integrate the system we use Euler method with five-node Laplacian operator, time step $\Delta t = 0.001$ and grid point spacing $\Delta x = 0.25$ (equivalent to 0.6 mm of physical space), $\epsilon = 0.0243$, $f = 1.4$, $q = 0.002$. The parameter ϕ characterizes excitability of the simulated medium: the medium is excitable and exhibits 'classical' target waves when $\phi = 0.05$ and the medium is subexcitable with propagating localizations, or wave-fragments, when $\phi = 0.0766$.

3 Ballistic of Physarum localizations

Proposition 1 *Given cross-junction of agar channels and plasmodium inoculated in one of the channels, the plasmodium propagates straight through the junction.*

We experimentally found that that plasmodium propagates under its own momentum when no gradients of repellents or attractants are applied. In example shown in Fig. 1a the plasmodium is inoculated in northmost part of the north-south channel. The plasmodium has the only option — to propagate south — because there is no gel substrate further north. Thus an internal 'momentum' is formed. No food sources are applied on the substrate to attract the plasmodium. The plasmodium propagates straightforwardly by itself. It does not

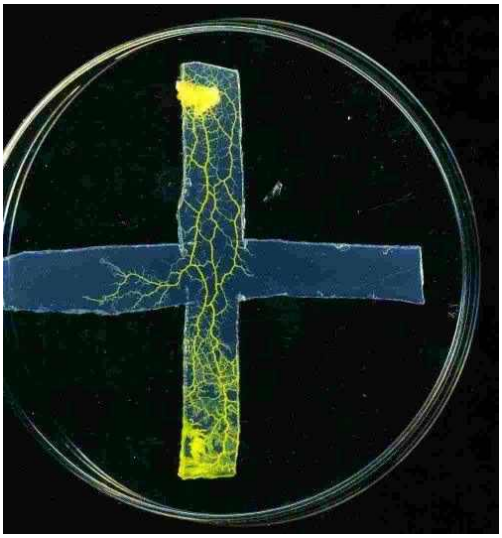

(a)

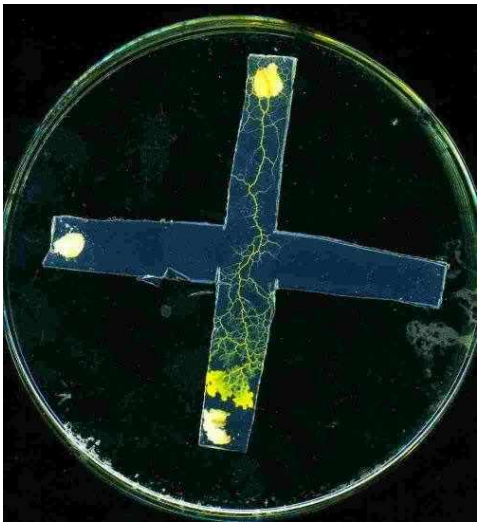

(b)

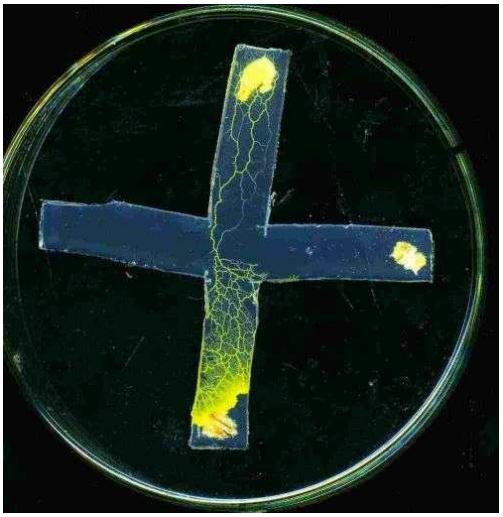

(c)

Fig. 1. Experimental examples of plasmodia moving under their own momenta: (a) no sources of chemo-attractants, (bc) oat flakes are placed in south and east (b), and south and west (c) ends of channels.

branch at the junction and moves till it reaches south end of the north-south channel (Fig. 1a).

In 21 out of 28 trials the plasmodium exhibits clear 'ballistic' behavior and propagates straight through the junction as under its own momentum. In 7 out of 28 trials the plasmodium turns into other channels or branches into several channels at once. Adding sources of attractants — assuming they are balanced over the channels (i.e. if there is an attractant in east-west channel there should be one in north-south channel) slightly speeds up propagation of plasmodium and does not change overall statistics of the plasmodium propa-

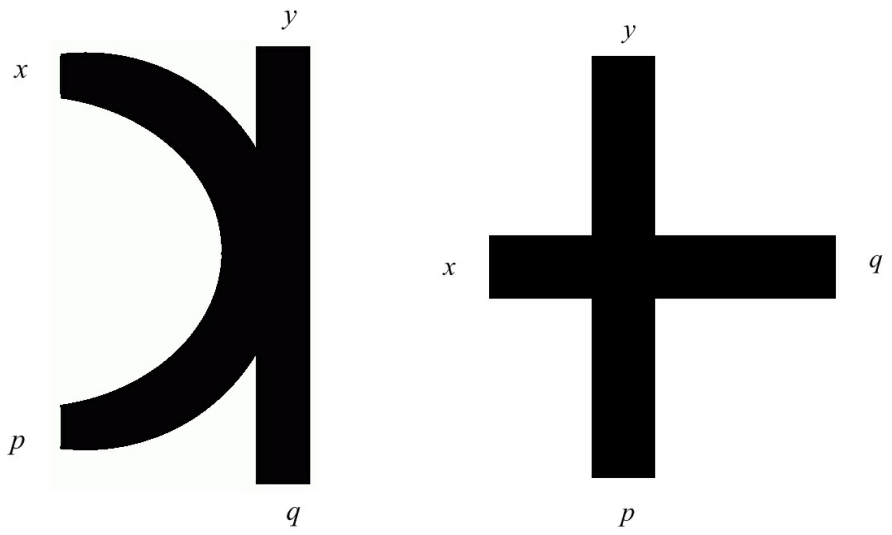

Fig. 2. Geometrical structure of Physarum gates P_1 (a) and P_2 (b): x and y are inputs, p and q are outputs.

gation. Examples are shown in Fig. 1b–d. Thus in experiments described in Sect. 4 we always used oat flakes to stimulate the plasmodium growth.

4 Physarum gates

Geometrical structure of gates P_1 and P_2 is shown in Fig. 2. We experimented with various shapes of agar and found that the most suitable templates are those shown in Fig. 2. Input variables are x and y and outputs are p and q. Presence of a plasmodium in a given channel indicates TRUTH and absence — FALSE.

Each gate implements a transformation from $\langle x, y\rangle \rightarrow \langle p, q\rangle$. Experimental examples of the transformations are shown in Fig. 3. Plasmodium inoculated in input y propagates along the channel yq and appears in the output q (Fig. 3a). Plasmodium inoculated in input x propagates till junction of x and y, 'collides' to the impassable edge of channel yq and appears in output q (Fig. 3b).

When plasmodia are inoculated in both inputs x and y they appear in both outputs p and q (Fig. 3c–e). In some cases plasmodia originated in different inputs avoid each other (Fig. 3cd) and thus head towards different outputs. In other cases the plasmodia merge in a single plasmodium but nevertheless branch towards different outputs (Fig. 3e). There are no strict rules on repelling and merging and often initial repelling between two plasmodia can be followed by merging (Fig. 3fg).

Typically for biological substrates, plasmodium of *Physarum polycephalum*

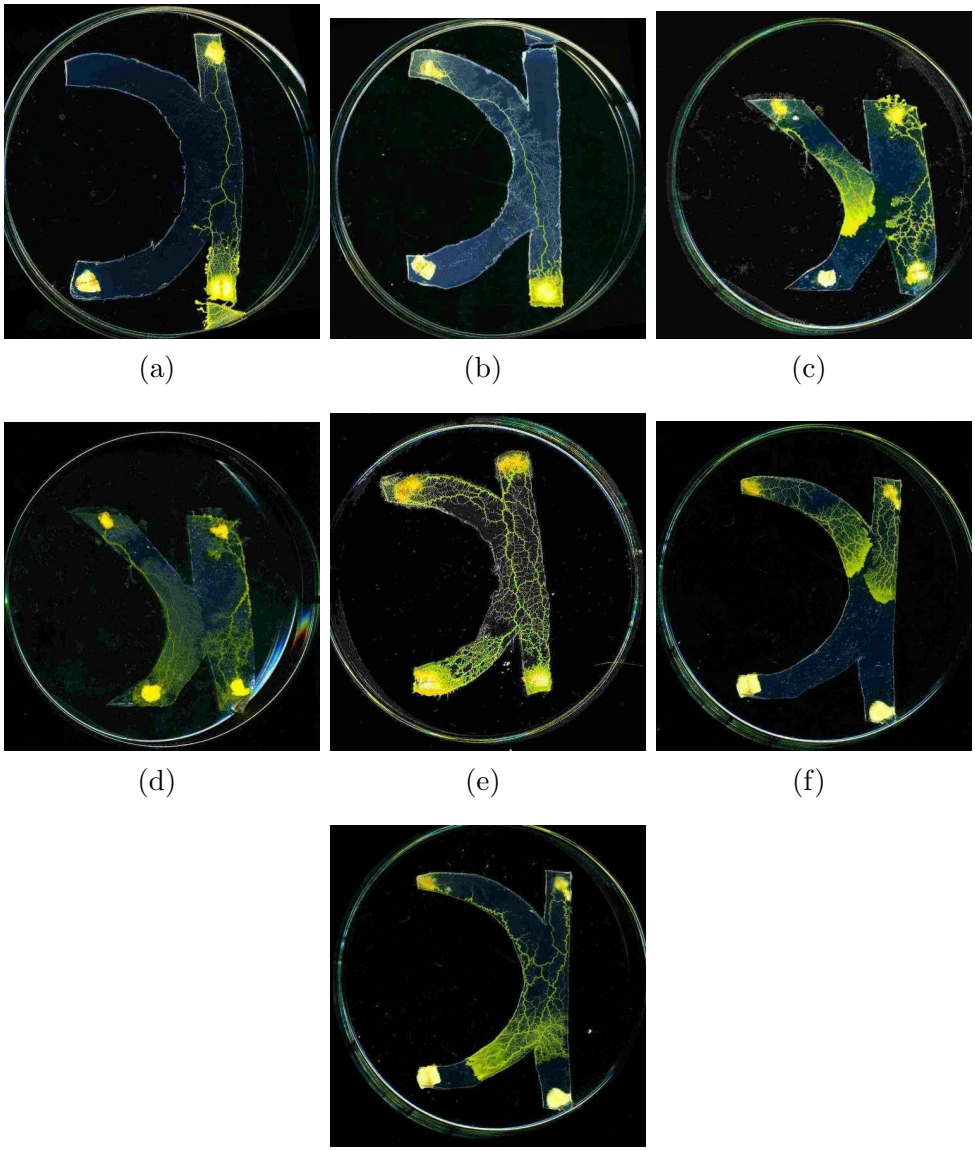

Fig. 3. Experimental examples of transformation $\langle x, y\rangle \to \langle p, q\rangle$ implemented by Physarum gate P_1. (a) $\langle 0, 1\rangle \to \langle 0, 1\rangle$, (b) $\langle 1, 0\rangle \to \langle 0, 1\rangle$, (c)–(e) $\langle 1, 1\rangle \to \langle 1, 1\rangle$. (f)–(g) snapshots of P_1 gate taken in 12 h interval.

is sensitive to experimental conditions. The plasmodium sometimes deviates from general scenario when implementing transformation $\langle x, y\rangle \to \langle p, q\rangle$. Results of experiments with Physarum gate P_1 are shown in Fig. 4a.

Plasmodia do not cancel each other at once. Therefore if at least one of the inputs is '1' we expect to see '1' at one of the outputs. Input scenario $\langle 1, 1\rangle$ is straightforward: in six out of seven experiments plasmodia appear on both outputs. Thus we obtain transformation $\langle 1, 1\rangle \to \langle 1, 1\rangle$ (Fig. 4a).

Plasmodium inoculated in input y (while input x is empty) will appear in

x	y	p	q	frequency
0	0	0	0	0
0	1	0	0	0
		0	1	$\frac{17}{22}$
		1	0	$\frac{2}{22}$
		1	1	$\frac{3}{22}$
1	0	0	0	0
		0	1	$\frac{9}{13}$
		1	0	$\frac{3}{13}$
		1	1	$\frac{1}{13}$
1	1	0	0	0
		0	1	$\frac{1}{7}$
		1	0	0
		1	1	$\frac{6}{7}$

(a)

x	y	p	q	frequency
0	0	0	0	0
0	1	0	0	0
		0	1	$\frac{4}{29}$
		1	0	$\frac{21}{29}$
		1	1	$\frac{4}{29}$
1	0	0	0	0
		0	1	$\frac{16}{27}$
		1	0	$\frac{5}{27}$
		1	1	$\frac{6}{27}$
1	1	0	0	0
		0	1	$\frac{13}{21}$
		1	0	$\frac{4}{21}$
		1	1	$\frac{5}{21}$

(b)

Fig. 4. Experimental data on transformations $\langle x, y\rangle \to \langle p, q\rangle$ implemented by Physarum gates (a) P_1 and (b) P_2. Values $x = 1$ and $y = 1$ are represented by plasmodia inoculated in inputs x and y, respectively. Values $p = 1$ and $q = 1$ are represented by plasmodia reaching outputs p and q, respectively. Frequency of each particular scenario $\langle a, b\rangle \to \langle c, d\rangle$ is presented by fraction: denominator is a total number of experiments for $\langle x, y\rangle = \langle a, b\rangle$ and numerator is a number of experiments completed with output tuple $\langle x, y\rangle = \langle c, d\rangle$.

output q in 17 out of 22 experiments. Thus the transformation $\langle 0, 1\rangle \to \langle 0, 1\rangle$ is realized by plasmodium in over 70%.

Input combination $\langle 1, 0\rangle$ gives us less stable results: in nine our of 13 experiments (69%) the plasmodium reaches output q. The plasmodium enters output p in three of 13 experiments, and the plasmodium branches inside both outputs in one experiment. Nevertheless the transformation $\langle 1, 0\rangle \to \langle 0, 1\rangle$ is realized by plasmodium in well over half of experiments (Fig. 4a).

Finding 1 *Plasmodium of* Physarum polycephalum *implements two-input two-output Boolean gate* $\langle x, y\rangle \to \langle xy, x + y\rangle$ *with reliability exceeding 69%.*

Experimental snapshots of plasmodium propagating in the gate P_2 are shown in Fig. 5. Taken input x is empty, plasmodium placed in input y usually (see statistics in Fig. 4) propagates directly towards output q (Fig. 5ab). Plasmod-

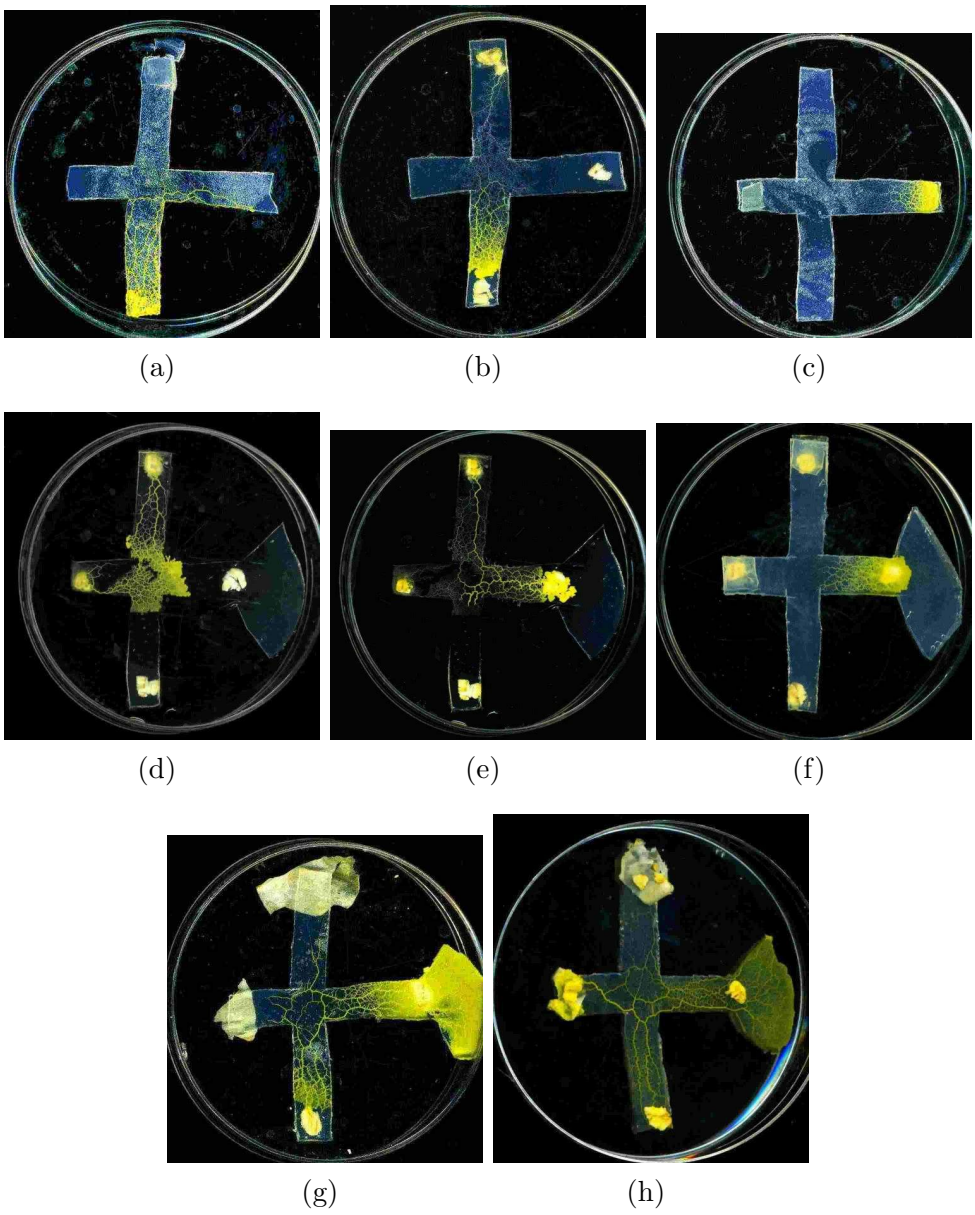

Fig. 5. Experimental examples of transformation $\langle x, y\rangle \to \langle p, q\rangle$ implemented by Physarum gate P_2: (a) $\langle 0, 1\rangle \to \langle 1, 0\rangle$, plasmodium is inoculated in input y, no oat flakes present; (b) $\langle 0, 1\rangle \to \langle 1, 0\rangle$, oat flakes are placed in both outputs; (c) $\langle 1, 0\rangle \to \langle 0, 1\rangle$, no oat flakes present; (d)–(e) two snapshots of transformation $\langle 1, 1\rangle \to \langle 0, 1\rangle$, taken with 11 h interval, oat flakes are placed in both outputs; (f) $\langle 1, 1\rangle \to \langle 0, 1\rangle$, oat flakes are placed in both outputs; (g)–(h) transformations $\langle 1, 1\rangle \to \langle 0, 1\rangle$ are less pronounced than in previous examples, however we see that output q is more extensively occupied by plasmodium than output p.

ium inoculated in input x (when input y is empty) travels directly towards output p (Fig. 5c). Thus transformations $\langle 0, 1\rangle \to \langle 1, 0\rangle$ and $\langle 1, 0\rangle \to \langle 0, 1\rangle$ are implemented.

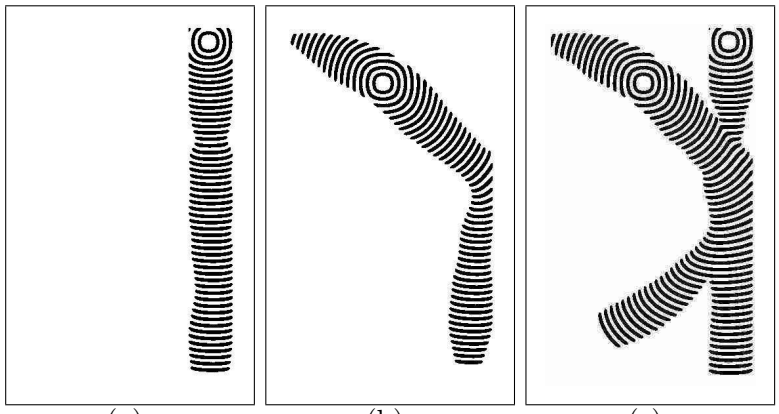

(a) (b) (c)

Fig. 6. Time lapsed images of localized excitations, wave-fragments, traveling in channels of gate P_1 filled with excitable medium. Dynamics of the excitable medium gate P_1 is shown during implementation of transformations (a) $\langle 0,1\rangle \to \langle 0,1\rangle$, (b) $\langle 1,0\rangle \to \langle 0,1\rangle$, (c) $\langle 1,1\rangle \to \langle 1,1\rangle$. The transformation $\langle 1,1\rangle \to \langle 1,1\rangle$ is simulated for initial excitations in channels x and y positioned at equal distance from their meeting point.

The gate's structure is asymmetric, x-channel is shorter than y-channel. Therefore the plasmodium placed in input x usually passes the junction by the time plasmodium originated in input y arrives at the junction (Fig. 5d–f). The y-plasmodium merges with x-plasmodium and they both propagate towards output q. Extension of gel substrate after output q does usually facilitate implementation of the transformation $\langle 1,1\rangle \to \langle 0,1\rangle$ (Fig. 5d–h).

Frequencies of various input-output transformations occurred in experiments are shown in Fig. 4b. Plasmodium inoculated in input y will reach only output p in 21 out of 29 experiments. Transformation $\langle 1,0\rangle \to \langle 0,1\rangle$ takes place in 16 out of 27 experiments. Transformation $\langle 1,1\rangle \to \langle 0,1\rangle$ occurs in 13 out of 21 experiments.

Finding 2 *Plasmodium of* Physarum polycephalum *implements two-input two-output gate* $\langle x,y\rangle \to \langle x,\overline{x}y\rangle$ *with reliability exceeding 59%.*

5 Simulation of Physarum gates

Experimental Findings 1 and 2 are confirmed in numerical simulation using two-variable Oregonator model of a sub-excitable medium (see Sect. 2). To represent value '1' in input channel x or channel y we generate an excitation near entrance of the channel. Two wave-fragments are formed. One travels outside the gate, another travels towards outputs.

Wave-fragments in sub-excitable media are notably unstable, they do keep

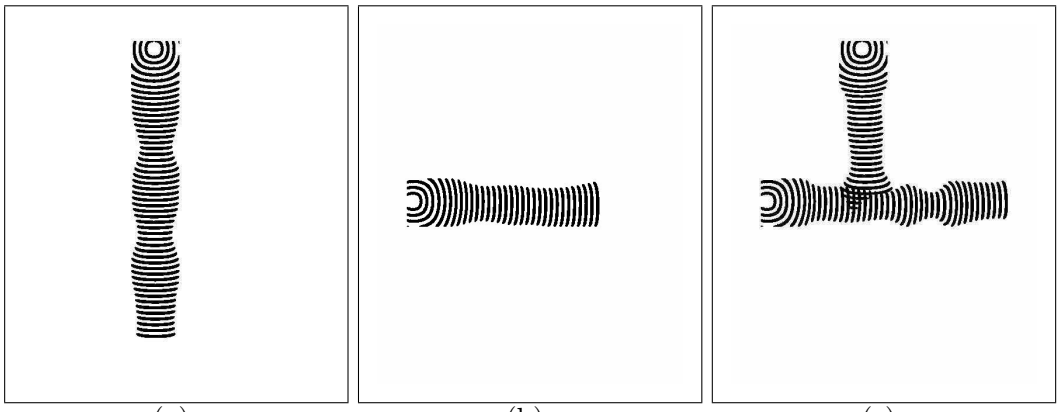

(a) (b) (c)

Fig. 7. Time lapsed images of localized excitations, wave-fragments, traveling in channels of gate P_2 filled with excitable medium. Dynamics of the excitable medium gate P_2 is shown during implementation of transformations (a) $\langle 0,1\rangle \rightarrow \langle 1,0\rangle$, (b) $\langle 1,0\rangle \rightarrow \langle 0,1\rangle$, (c) $\langle 1,1\rangle \rightarrow \langle 0,1\rangle$.

their shape only for a short period of time. Then the fragments either shrink and annihilate or expand unlimitedly. During simulation of gates P_1 and P_2 we manually adjusted parameter ϵ (see Sect. 2) to keep wave-fragments from collapsing and expanding. Figures 11 and 12 illustrate dynamics of ϵ during simulations of gates P_1 (Fig. 6) and P_2 (Fig. 7).

Let us look at the time lapsed images of wave-fragments propagating in gate P_1 (Fig. 6) and gate P_2 (Fig. 7). Scenarios where only one input is excited are straightforward. When $y = 1$ in gate P_1 is initialized the wave-fragment propagates southward along the channel yq (Fig. 6a). Wave-fragment initiated in input x ($x = 1$) of gate P_1 propagates along input channel x and collides to the boundary of channel yq (Fig. 6b). The wave-fragment recovers after collision to the boundary, travels along the channel yq and appears in the output q (Fig. 6b). Wave-fragments behave similarly in situations of input tuples $\langle 1,0\rangle$ and $\langle 0,1\rangle$ in gate P_2. They propagate straight along their original input channel and reach outputs opposite to their entry points (Fig. 7ab).

In input scenarios $\langle 0,1\rangle$ and $\langle 1,0\rangle$ size of propagating wave-fragment was not enough for the fragment to branch into output channel p of gate P_1 (Fig. 6ab). When two wave-fragments are initiated, $x = 1$ and $y = 1$, they collide at the junction of input channels x and y. The wave-fragments merge into a single larger-wave fragment. This new fragment propagates towards output q and also expands into output channel p (Fig. 6c).

In gate P_2, inputs $x = 1$ and $y = 1$, wave-fragment originated in x-input arrives at the junction between channel xp and yq a bit earlier then wave-fragment originated in y-input. Therefore y-wave collides into refractory tail of x-wave. The y-wave annihilates (Fig. 7c). Such development is phenomeno-

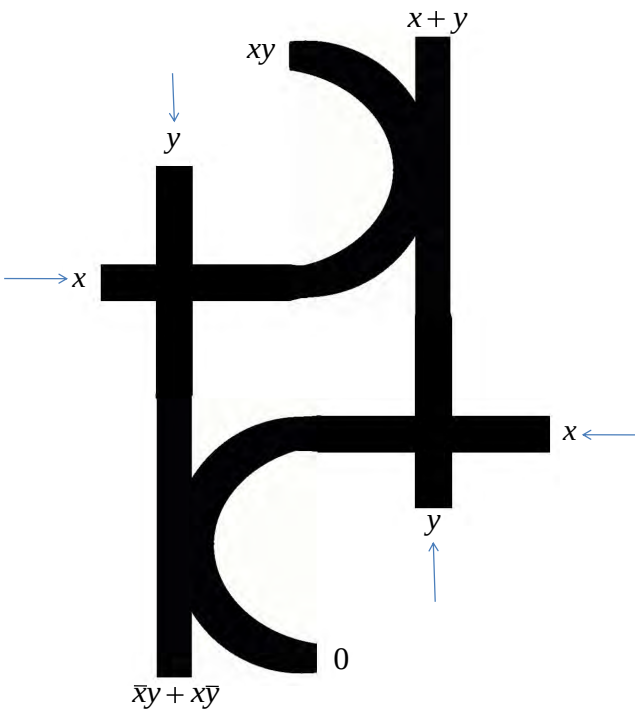

Fig. 8. Scheme of one-bit half-adder made of gates P_1 and P_2. Inputs are indicated by arrows. Outputs $\overline{x}y + x\overline{y}$ and xy are sum and carry values computed by the adder. Outputs 0 and $x + y$ are byproducts.

logically identical to Physarum gate P_2 (Fig. 5de) with the only difference that plasmodium 'wave' originated in input y is not annihilated but merges with plasmodium originated in input x.

6 Simulated one-bit half-adder

One-bit half-adder is a logical circuit which takes two inputs x and y and produces two outputs: sum $\overline{x}y + x\overline{y}$ and carry xy. To construct a one-bit half-adder with Physarum gates we need two copies of gate P_1 (Fig. 2a) and two copies of gate P_2 (Fig. 2b). Cascading the gates into the adder is shown in Fig. 8. Signals x and y are inputted in P_2 gates. Outputs of P_2 gates are connected to inputs of P_1 gates.

We did not manage to realize one-bit half-adder in experiments with living plasmodium because the plasmodium behaved differently in the assembly of the gates than in isolated gates. Simulation of the adder using Oregonator model was successful (Fig. 9). To simulate inputs $x = 0$ and $y = 1$ we initiate wave-fragments at the beginning of channels, marked y and arrow in Fig. 8. The wave-fragments propagate along their channels. The waves do not branch at the junctions with other channels because we keep the wave-fragments

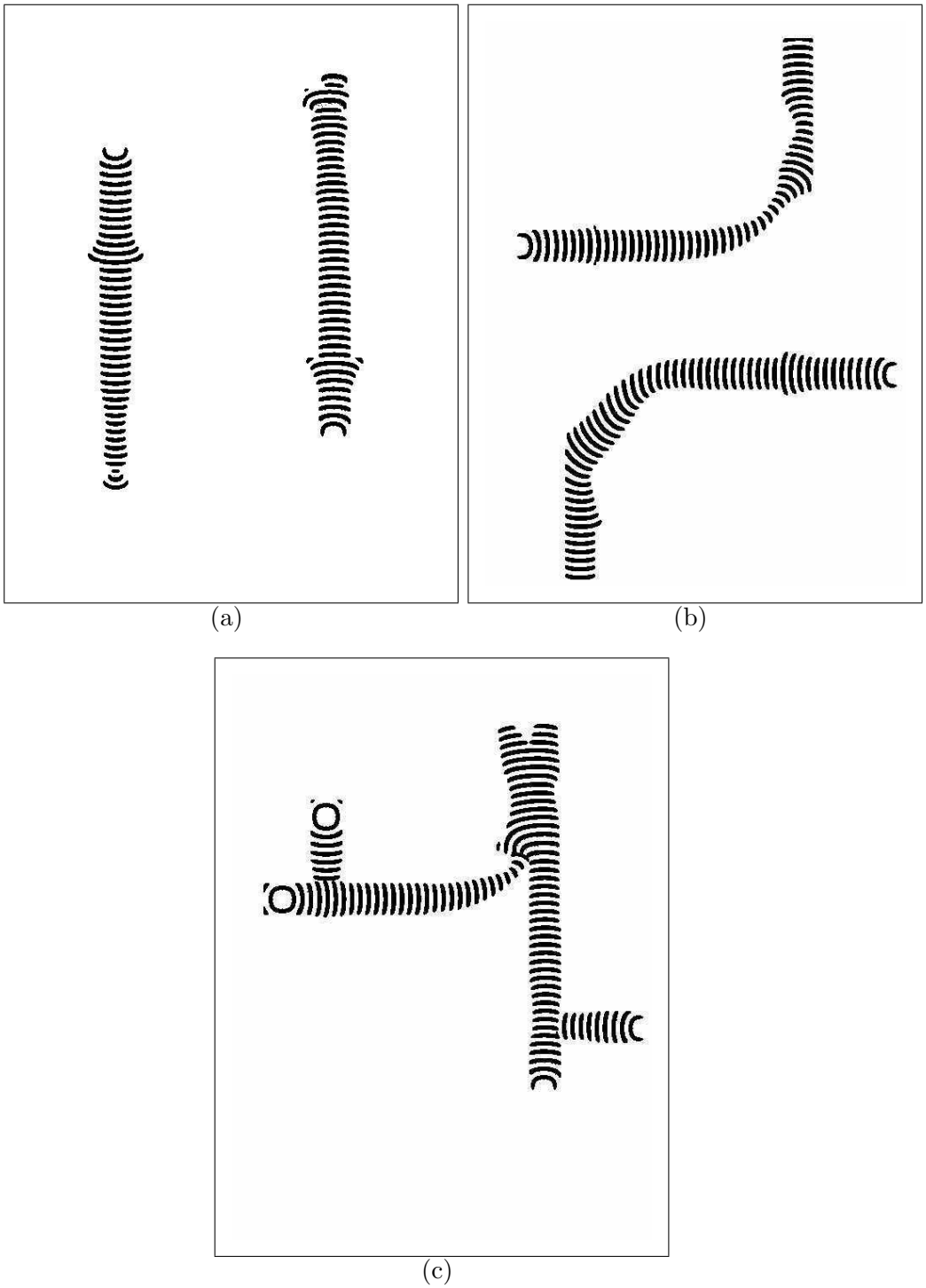

Fig. 9. Time lapsed images of localized excitations, wave-fragments, traveling in channels of one-bit half-adder filled with excitable medium. Dynamics of excitations is shown for input values (a) $x = 0$ and $y = 1$, (b) $x = 1$ and $y = 0$, (c) $x = 1$ and $y = 1$.

localized by varying parameter ϵ (Fig. 9a).

For input values $x = 1$ and $y = 0$ wave-fragments are originated in sites marked x and arrow in Fig. 8. The wave-fragment started in left x-input channel propagates towards $x + y$-output of the adder. The wave-fragment originated in right x-input channel travels towards $\overline{x}y + x\overline{y}$ (Fig. 9b).

When both inputs are activated, $x = 1$ and $y = 1$, wave-fragment originated in left y-input channel is blocked by refractory tail of wave-fragment originated in left x-input channels. The wave-fragment traveling in right x-input channel is blocked by tail of wave-fragment traveling in right y-input channel. The wave-fragments representing $x = 1$ and $y = 1$ enter top-right gate P_1 and emerge at its outputs xy and $x + y$ (Fig. 9b). Thus functionality of the circuit Fig. 9 is demonstrated.

7 Discussion

We established experimentally and in numerical simulations that plasmodium of *Physarum polycephalum* realizes basic logical operations on a geometrically-constrained non-nutrient substrate. We designed two types of Boolean logic gates, both gates have two inputs and two outputs. The gates implement transformations $\langle x, y\rangle \to \langle xy, x + y\rangle$ and $\langle x, y\rangle \to \langle x, \overline{x}y\rangle$. We shown how the Physarum gates can be assembled into a one-bit half-adder. Functionality of the adder is illustrated using two-variable Oregonator model.

Our designs are based on the interactions between traveling localizations: plasmodium localizations propagating on a non-nutrient substrate and wave-fragments propagating in a sub-excitable medium. Similarities between the plasmodium localizations and wave-fragments are discussed in details [6]. We stress that things go absolutely differently on a nutrient-rich substrate (corn meal agar) and fully excitable chemical medium. Plasmodium inoculated in any point of the nutrient-agar gel gate propagates in all channels (Fig. 10a–c). An excitation wave initiated at any point of excitable medium gate spreads all over the gate (Fig. 10d). We can conclude therefore that it is impossible to implement logical functions with plasmodium of *Physarum polycephalum* on a nutrient-rich substrate.

Reliability of experimental Physarum gate is quite low: 69% for gate P_1 and 59% for gate P_2. This is because behavior of plasmodium is determined by too many environmental factors — thickness of substrate, humidity, diffusion of chemo-attractants in the substrate and in the surrounding air volume, and physiological state of plasmodium during each particular experiment. Increasing reliability of Physarum gates might be a scope of further studies.

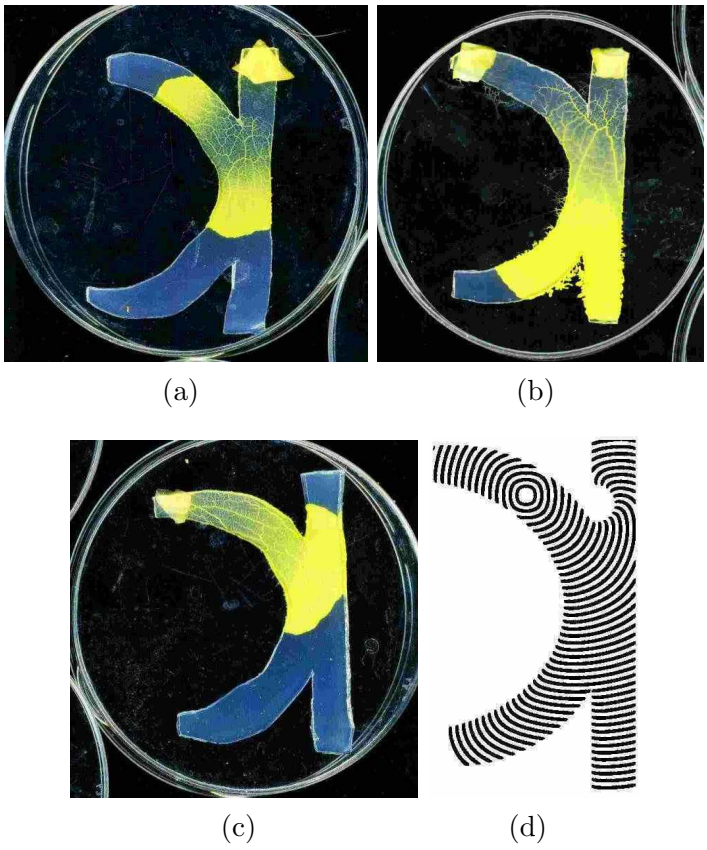

Fig. 10. Snapshots of plasmodium propagating in gate P_1 on 2% corn meal agar (a–c) and numerical simulation (d): (a) inputs $x = 0$ and $y == 1$, see the gate's scheme in Fig. 2, (b) inputs $x = 1$ and $y = 1$, (c) inputs $x = 1$ and $y = 0$, (d) time lapsed images of excitation wave propagating in gate P_1 for inputs $x = 1$ and $y = 0$, simulation of case (c).

References

[1] Adamatzky, A. Computing in nonlinear media and automata collectives, CRC Press (2001).

[2] Adamatzky A. (ed.). Collision-Based Computing. Springer, London, 2002.

[3] Adamatzky A. Collision-based computing in Belousov–Zhabotinsky medium. Chaos Solitons Fractals 21 (2004) 1259–1264.

[4] Adamatzky, A. Physarum machine: implementation of a Kolmogorov-Uspensky machine on a biological substrate. Parallel Processing Letters 17 (2007) 455–467.

[5] Adamatzky A. Developing proximity graphs by Physarum Polycephalum: Does the plasmodium follow Toussaint hierarchy? Parallel Processing Letters 19 (2008) 105–127.

[6] Adamatzky A., De Lacy Costello B., Shirakawa T. Universal computation

with limited resources: Belousov-Zhabotinsky and Physarum computers. Int. J. Bifurcation and Chaos 18 (2009) 2373–2389.

[7] Adamatzky A. If BZ medium did spanning trees these would be the same trees as Physarum built. Physics Letters A 373 (2009) 952–956.

[8] Beato V., Engel H. Pulse propagation in a model for the photosensitive Belousov-Zhabotinsky reaction with external noise. In: Noise in Complex Systems and Stochastic Dynamics, Edited by Schimansky-Geier L., Abbott D., Neiman A., Van den Broeck C. Proc. SPIE 2003 (5114) 353–362.

[9] De Lacy Costello B. and Adamatzky A. Experimental implementation of collision-based gates in Belousov-Zhabotinsky medium. Chaos, Solitons and Fractals 25 (2005) 535–544.

[10] Field R. J., Noyes R. M. Oscillations in chemical systems. IV. Limit cycle behavior in a model of a real chemical reaction. J. Chem. Phys. 1974 (60) 1877–1884.

[11] Nakagakia T., Yamada H., Ueda T. Interaction between cell shape and contraction pattern in the *Physarum plasmodium*, Biophysical Chemistry 84 (2000) 195–204.

[12] Nakagaki T., Smart behavior of true slime mold in a labyrinth. Research in Microbiology 152 (2001) 767-770.

[13] Nakagaki T., Yamada H., and Toth A., Path finding by tube morphogenesis in an amoeboid organism. Biophysical Chemistry 92 (2001) 47-52.

[14] Nakagaki T., Iima M., Ueda T., Nishiura y., Saigusa T., Tero A., Kobayashi R., Showalter K. Minimum-risk path finding by an adaptive amoeba network. Physical Review Letters 99 (2007) 068104.

[15] Saigusa T., Tero A., Nakagaki T., Kuramoto Y. Amoebae anticipate periodic events. Phys Rev Lett. 2008 (100) 018101.

[16] Shirakawa T., Adamatzky A., Gunji Y.-P., Miyake Y. On simultaneous construction of Voronoi diagram and Delaunay triangulation by Physarum polycephalum. Int. J. Bifurcation and Chaos 19 (2009) 31093117.

[17] Tsuda S., Aono M., Gunji Y.-P. Robust and emergent Physarum logical-computing. Biosystems 73 (2004) 45–55.

[18] Tsuda S, Zauner K.-P., Gunji Y.-P. Robot control with bio-logical cells. BioSystems 87 (2007) 215–223.

Appendix A

Figures 11 and 12 show how parameter ϵ (see description of the model in Sect. 2) is changed during simulation of gates P_1 and P_2 in a sub-excitable medium. We also show dynamics of the medium's activity. At each step of simulation we calculate activity $\alpha^t = |\mathbf{L}|^{-1} \cdot \sum_{x \in \mathbf{L}} u_x^t$ as a sum of values u for each node of the grid $\mathbf{L}$ normalized by total number of nodes $|\mathbf{L}|$.

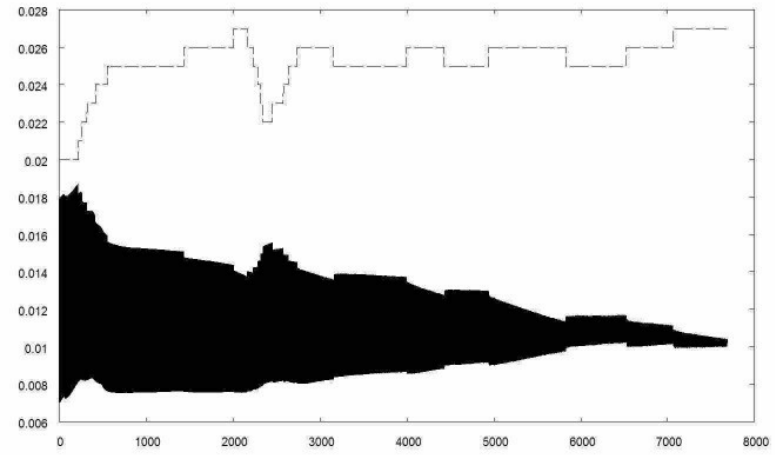

(a)

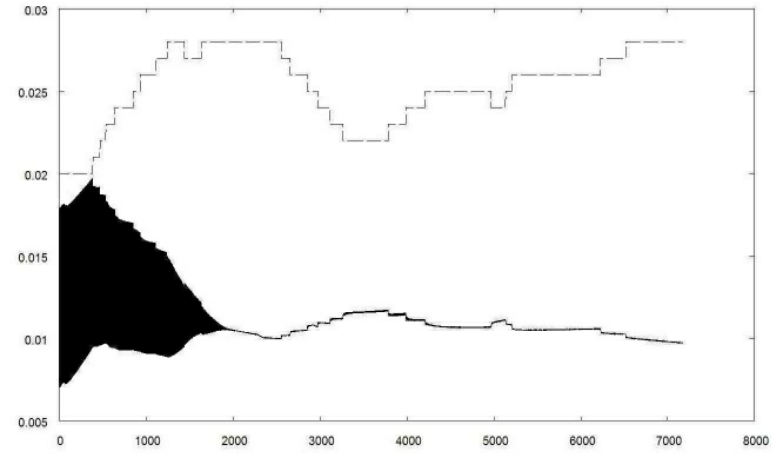

(b)

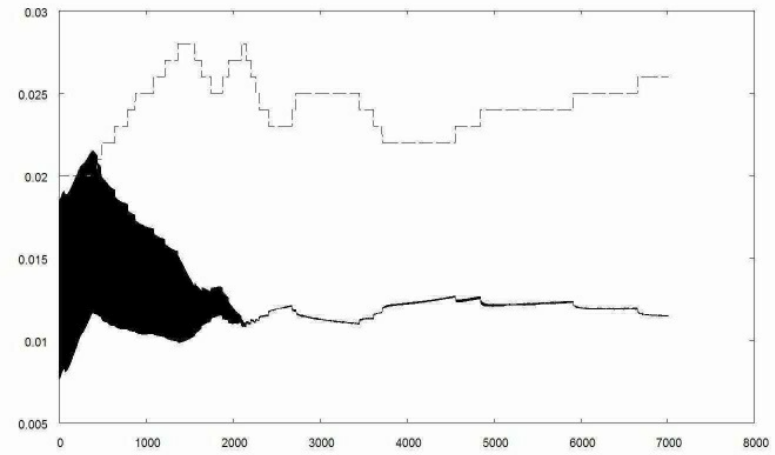

(c)

Fig. 11. Dynamics of parameter ϵ, dotted line, and activity α, solid line, during operation cycle of gate P_1 for input tuples (a) $\langle 0,1\rangle$ (see Fig. 6a), (b) $\langle 1,0\rangle$ (see Fig. 6b), (c) $\langle 1,1\rangle$ (see Fig. 6c).

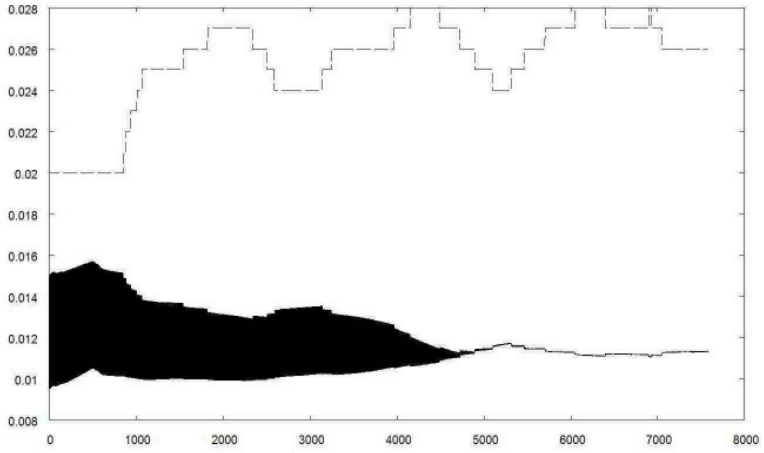

(a)

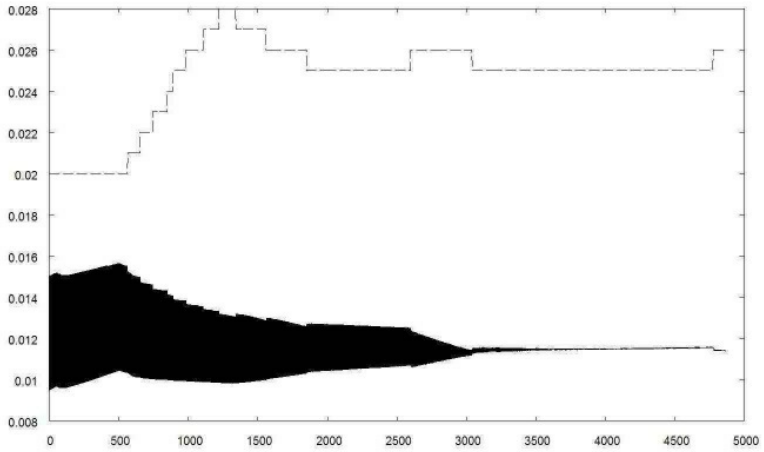

(b)

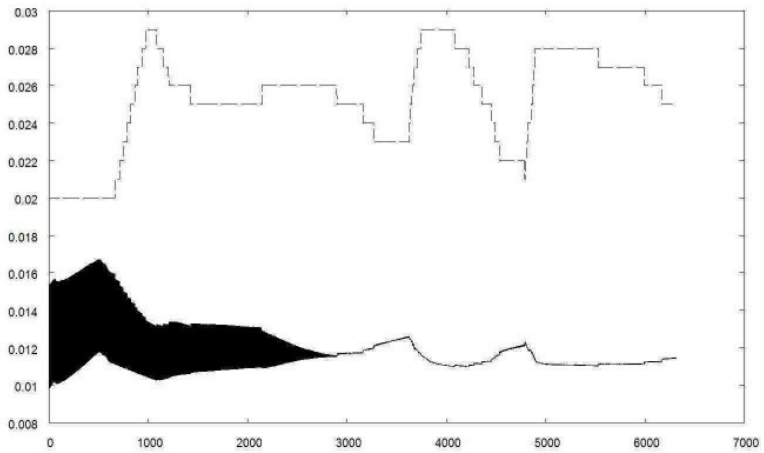

(c)

Fig. 12. Dynamics of parameter ϵ, dotted line, and activity α, solid line, during operation cycle of gate P_2 for input tuples (a) $\langle 0,1\rangle$ (see Fig. 7a), (b) $\langle 1,0\rangle$ (see Fig. 7b), (c) $\langle 1,1\rangle$ (see Fig. 7c).

View publication stats